OPEN ACCESS
Journal of Innovative Optical Health Sciences
Vol. 16, No. 2 (2023) 2244002 (12 pages)

DOI: 10.1142/S1793545822440023

World Scientific
www.worldscientific.com

Suppression of transmembrane sodium currents on the freshly isolated hippocampal neuron cell with continuous infrared light

Fanyi Kong*, Xinyu Li†, Ruonan Jiao*, Kun Liu*, Xue Han*, Changkai Sun‡ and Changsen Sun*,§

*School of Optoelectronic Engineering and Instrumentation Science
Dalian University of Technology
No. 2 Linggong Road, High-tech Zone
Dalian 116024, P. R. China

†School of Electronics and Information Technology
Yat-sen University, No. 135 Xingang Xi Road
Guangzhou 510006, P. R. China

‡School of Biomedical Engineering
Dalian University of Technology
No. 2 Linggong Road, High-Tech Zone
Dalian 116024, P. R. China
§suncs@dlut.edu.cn

Received 19 February 2022
Revised 21 May 2022
Accepted 22 May 2022
Published 12 October 2022

Physiotherapeutic effects of infrared lasers have been proved in clinic. These infrared-based regulations of the bioelectrical activities can roughly be classified into enhancement and suppression of action potential (AP), which are described by sodium (Na) and potassium (K) transmembrane current equations, named as Hodgkin and Huxley (HH)-model. The enhancement effect is able to evoke or strengthen the AP when infrared light is applied. Its corresponding mechanism is commonly ascribed to the changes of the cell membrane capacitance, which is transiently increased in response to the infrared radiation. The distinctive feature of the suppression effect is to inhibit or reduce the AP by the designed protocols of infrared radiation. However, its mechanism presents more complexity than that in enhancement cases. HH-model describes how the Na current determines the initial phase of AP. So, the enhancement and suppression of AP can be also ascribed to the regulations of the corresponding Na currents. Here, a continuous infrared light at the wavelength of 980 nm (CIS-980) was employed to stimulate a freshly isolated hippocampal neuron *in vitro* and a suppression effect on the Na currents of the neuron cell was observed. Both Na and K currents, which are named as whole cell currents, were simultaneously recorded with the cell membrane capacitance current by using a patch clamp

combined with infrared irradiation. The results demonstrated that the CIS-980 was able to reversibly increase the capacitance currents, completely suppressed Na currents, but little changed K currents, which forms the steady outward whole cell currents and plays a major role on the AP repolarization. A confirmation experiment was designed and carried out by synchronizing tens of milliseconds of infrared stimulation on the same kinds of hippocampal neuron cells. After the blocked K channel, a reduction of Na current amplitude was still recorded. This proved that infrared suppression of Na current was irrelevant to K channel. A membrane capacitance mediation process was preliminarily proposed to explain the Na channel suppression process.

Keywords: Na channel suppression; AP; whole cell currents; infrared suppression of bioelectrical activity; photothermal effect on the membrane capacitance; continuous infrared laser physiotherapy.

1. Introduction

Infrared therapy had shown its abilities in clinic, such as diabetic wounds repair,[1,2] pain relief,[3] auditory response stimulation,[4,5] and the recent achievement in brain–computer interfaces.[6] The most interesting work is controlling the nerves' bioelectrical functions without any pretreatment on the biological samples,[7] which is the cellular basis of the most infrared therapies, laser acupuncture in clinic, etc. The studies on their corresponding cellular mechanisms can be classified into two categories according to their roles of enhancement or suppression for the action potential (AP), which are described by Na and K transmembrane current equations developed by Hodgkin and Huxley (HH)[8] in 1952 and named as HH-model. And these contents can be easily obtained in the textbooks about Cellular Electrophysiology or Cellular Biophysics, etc.

HH-model[8] provided a set of quantitative description equations for ionic transmembrane currents flowing through ion-selective channels on the excitable cell membrane and formed a biophysical branch thereafter. This model made a clear understanding of the AP of the excitable cell membrane. It says that the initial phase of the AP is initiated by a rapid voltage-dependent inward Na current. And its recovery phase is formed by a slowly voltage-dependent outward-rectifier K current. The Na and K currents make a shape of whole cell current, which describes the AP on the ionic basis.

The functional enhancement roles had been studied based on the infrared-induced activation of ionic channel,[9] AP,[10,11] etc., but its mechanism was kept unclear until Shapiro *et al.* proposed a membrane capacitance mediation principle.[12] This capacitive mechanism is described as follows: Laser-induced thermal effect increased membrane capacitance, generated an inward capacitive current, then depolarized the cell membrane, and finally evoked an AP. They proved that the membrane capacitance was mediated by the infrared laser regulation on the cell bioelectrical activities. Based on this mechanism, we studied the enhancements also.[13,14] Thereafter, the works demonstrated that these capacitance changes were determined by the "thermostriction" of the lipid bilayer in a rapid temperature change induced by the photothermal effect.[15–17]

On the other hand, the infrared lasers have also been found to be able to suppress cellular electrical activation when operated in an appropriate way.[18–20] The transient and selective infrared suppressions of neuron activity were proved in relation to the localized heating block. But, its mechanism was not as clear as that of enhancement,[21] even if the novel methods had been employed such as nanoparticle methods.[22,23] The consideration of the different temperature sensitivity of the membrane protein (Q_{10})[24] was proposed based on the modified HH model.[25]Along with this clue, Ganguly *et al.*[26] proposed that the mechanism of K channel played a major role during the infrared inhibition. Anyway, these publications demonstrated bidirectional regulation roles of the infrared light on the AP. And technically, the patch clamp provided a tool for the whole cell currents or AP recording.[27] So, the Na and K currents could act as a quantitative measure to understand the infrared physiotherapeutic effect as shown in Refs. 9, 12–14, 18, 19, and 33.

Here, we present an observation of a long-term infrared suppression phenomenon on the freshly isolated hippocampal neuron cell and propose its mechanism as a slow changing membrane capacitance mediation. A Patch Clamp technique was applied to synchronize an infrared laser to study how a hippocampal neuron cell responds to a CIS-980 irradiation *in vitro*.

We preliminarily proposed a mechanism where a CIS-980 suppression of transmembrane Na currents was mediated by membrane capacitance. The laser-induced photothermal effect generated a slow temperature rises (compared with the rapid pulsed laser), induced an inward capacitance current, increased the membrane potential, and then caused Na channel suppression (this is also called deactivation process) like applying a ramp depolarization voltage, and consequently, the cellular level Na current(s) were suppressed. Finally, the opinions on infrared suppression of AP from the other groups were discussed.

2. Neuron Cell Preparation and Methods

2.1. *Hippocampal neurons preparation*

The animal treatment procedures used in this study adhered to the tenets of the Biological and Medical Committee of Dalian University of Technology (No. 20190701). Approval was granted by the Institutional Animal Care and Use Committee. Animals were provided by the Animal Center of Dalian Medical University, Dalian, China.

Hippocampal neurons were prepared from 7 to 10-day-old Spraque Dawley rats in a conventional operation.[28] The brain was separated and then the hippocampus was dissected in cold Krebs buffer (5°C). Small pieces with about 0.5 mm thickness were cut from the tissue. Pronase E was added with a concentration of 1.5 g/L to those pieces for 20 min after the incubation at 32°C for 90 min. The tissue was then washed thrice with a calcium(Ca)-free solution, followed by washing with the Ca-containing solution thrice. Individual neurons were separated mechanically by lightly beating with a pasteurized glass pipette. Ca-free solution (mM) was composed of 150 NaCl, 5 KCl, 1.2 KH_2PO_4, 1.3 $MgSO_4$, 2 Ethylenebis(oxyethylenenitrilo)tetraacetic acid (EGTA), 26 $NaHCO_3$, 10 Glucose (pH = 7.4).

2.2. *Methods*

2.2.1. *Infrared stimulation setup and description*

The light source in our work is a Laser Diode Combi Controller ITC510 (Thorlabs, USA) with a 980 nm light unit (LU0980M180, Lumics, Germany), which works in a modulated mode.[13] We use a single-mode optical fiber with 10 μm core diameter and 125 μm external diameter to transfer the infrared laser light to cell surface. The schematic and the photothermal distribution are shown in Fig. 1. The time synchronization of laser controller and EPC-10 patch clamp is set in PULSE software (HEKA, Germany) at a time accuracy of 0.1 ms. Laser powers calibrated by PM100 power meter (Thorlabs, USA) were set at 30 and 72 mW for the long-term and short-term stimulations, respectively. The stimulation fiber was fixed at an angle of 60° to the horizontal plane, and the geometric relationship between fiber and neuron cell is shown in Fig. 1(a), in which the axial distance (z) and the spot radius (ω) at the neuronal level were calculated as ~108 μm and ~16.2 μm, respectively, where the spot radius is estimated by $\omega = 5 + 108^{*}\tan\alpha = 16.2$, in which α is the divergent angle determined by the numerical aperture (NA) of optical fiber , which can be calculated as: $\mathrm{NA} = n_0 \sin\alpha = 0.15$ with the fiber refractive index $n_0 = 1.47$. Based on the above parameters, the optical power density in space corresponding to 72-mW optical power used in this experiment can be calculated as follows:

$$72/[\pi \times 16.2^2] \approx 87.3 \times 10^3\,\mathrm{mW/mm^2}.$$

The thermal field generated by CIS-980 is commonly described by a thermal lens as given in Refs. 29–31 as follows:

$$\Delta T(r,t) = [2\mu_a P \exp(-\mu_a z)]/c\pi\omega^2(z) \int_0^t \frac{1}{1+\frac{2t'}{t_c}} \times \exp\left[-\frac{2r^2}{\omega^2\left(1+\frac{2r}{t_c}\right)}\right] dt' \quad (t < t_L), \tag{1}$$

where ΔT is the temperature changes. The characteristic time of thermal lens[31] t_c is expressed as $\omega^2/4D$, where D is water diffusion constant $1.43 \times 10^{-7}\,\mathrm{m^2/s}$. With a given laser power P, total stimulation duration t_L and water parameters[32] (optical absorption coefficient $\mu_a = 0.502\,\mathrm{cm^{-1}}$, water density ρ, dielectric

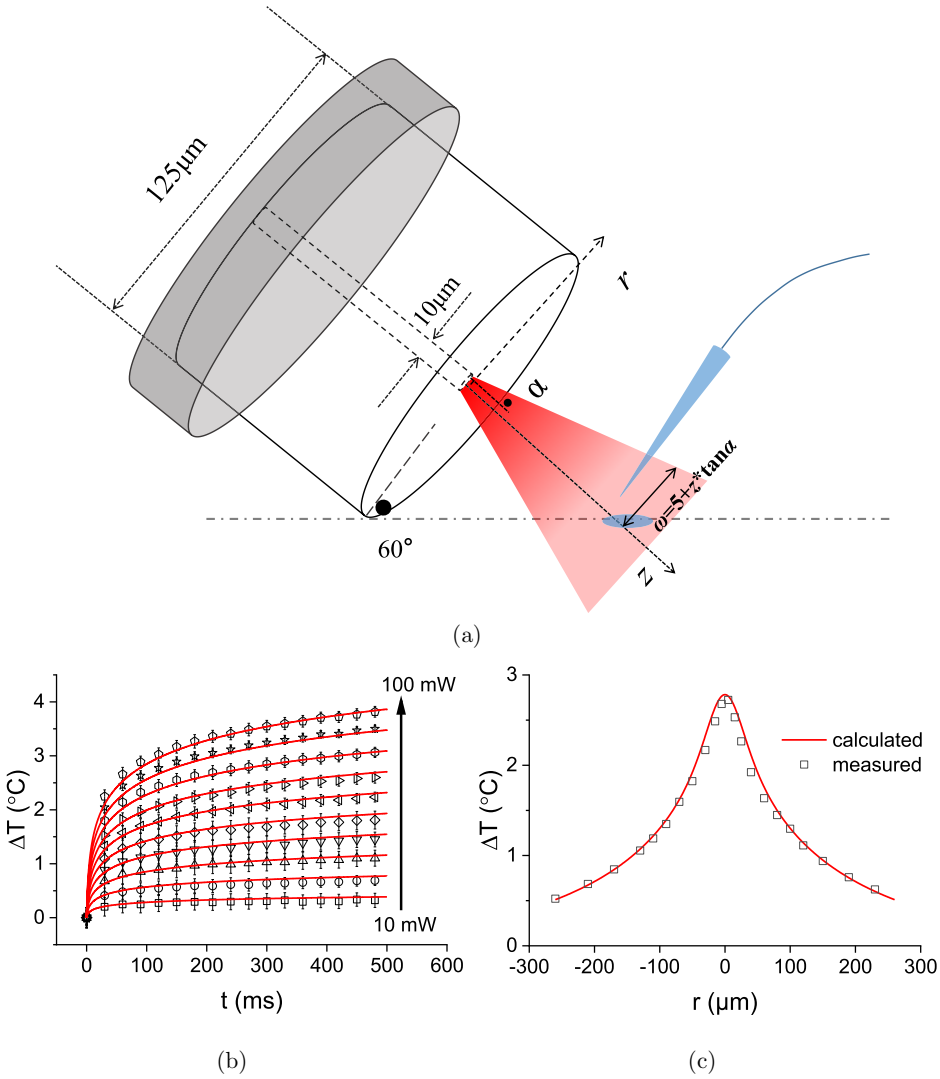

Notes: (a) The geometric relationship between the end of fiber and neuron cell (blue). (b) and (c) The measured (points) and calculated (curves) temperature changes based on Eq. (1) at $z = 300\,\mu$m. Points in (b) were measured temperature changes by using open pipette method at $r = 0$ ($p = 10$–100 mW) varying according to time t, which began from the infrared being applied, and data in (c) were the temperature changes measured at different r after 500 ms irradiation, respectively.

Fig. 1. The schematic and the photothermal distribution of the infrared light interaction with the neuron cell *in vitro*.

constant c), ΔT can be calculated and is shown in Figs. 1(b) and 1(c) as red curves.

In addition to the above calculation of the thermal field, Yao *et al.*[33] proposed a method to measure this infrared-induced temperature increase by using an open pipette method. And a simplified description of the relationship between the surrounding temperature T and the pipette current I had been set up as follows:

$$T = \frac{1}{\frac{1}{T_0} - \frac{R}{Ea}\log\left(\frac{I}{I_0}\right)}, \qquad (2)$$

where R is the gas constant and E_a is the activation energy, which is determined by the pipette current I_0 at initial temperature T_0.

We also practically measured the temperature distribution by using this open pipette method. The solution temperature was controlled from 25°C to 55°C and increased in a step of 1°C by using a thermostatic controller (tc-324b, Warner). Thirty-one traces of open pipette currents with 100 mV excitation voltages were recorded underlying each temperature. We reconstructed the temperature field distribution by moving the tip of the micro-open pipette and matched the calculated results

given in Figs. 1(b) and 1(c). This detailed work can be found in Ref. 14 and we display some results to illustrate how the temperature changes during the infrared laser irradiation.

2.2.2. *The membrane capacitance and ionic currents recording*

This part made a mini review on the related methods in convenience of readers from different fields. A commercialized Patch Clamp technique had been employed to record the membrane capacitance and ionic currents underlying an infrared stimulation. The infrared stimulation was synchronized by Patch Clamp as described in Refs. 13 and 14.

The glass pipette was prepared by a PC-10 vertical microelectrode drawing machine (NARISHIGE, Japan). The pipette tip was in the diameters of several micrometers and attached the cell membrane to form a seal of gigaohm. Patch electrode resistance was around 3–5 megaohm. After breaking the cell membrane on almost the top of the cell body by the tip through applying a negative gas pressure, the pipette connected with the inner cellular solution and formed a close circuit with the grounded extracellular solution.

The Na current(s) recording in this experiment were done in the whole-cell mode with an EPC-10 amplifier driven by PULSE software (HEKA, Germany). Signals were filtered at 2.9 kHz and sampled at 50 kHz. The patch pipette was controlled by a three-dimensional MX7600 motorized micromanipulator with a MC1000e controller (SD Company). The neuron was housed in a recording chamber mounted on top of an Olympus IX 71 inverted microscope. Capacitance compensations were set in manual compensation mode in the interface of the PULSE.

Pipette solution (mM) is composed of 65 KCl, 80 KF, 5 KOH, 2 Na_2ATP, 10 EGTA, 10 HEPES. Tric-HCl is used to adjust solution pH to 7.4 (6 mM/L Tetraethylammonium was added for short-term experiment). Bath solution (mM) is composed of 150 NaCl, 5 KCl, 1.1 $MgCl_2$, 2.6 $CaCl_2$, 10 HEPES, 10 Glucose. Tric-HCl is used to adjust solution pH to 7.4.

EPC-10 capacitance compensation is an inserted function, which can be activated by operating the software. The normal role of the capacitance compensation is to cancel the membrane capacitance current to record an undisturbed Na current. Here, in order to observe the relationship between the membrane capacitance current and Na current, we employed this function to carry out a simultaneous measurement of the capacitance current and Na current by fine controlling the capacitance compensation in a slightly less magnitude. We chose capacitance compensation in a manual way because C_{slow} compensation is used presumably, it must cancel some of the capacitance present in the stimulus pathway, otherwise that must cause ambiguity in the following capacitance calculation.

In whole-cell recording mode, a compensation capacitive current is applied by EPC-10 amplifier in an opposite direction of the real membrane capacitance current to reduce its amplitude in a larger part, in order to record an unambiguous rapid Na current, which is immediately after the capacitive current. The compensation capacitive current is generated by the amplifier based on the "C-Slow" compensation. This is a common method to measure both cell membrane capacitance and ion currents simultaneously. The compensation principle was described in the EPC-10 operation manual for the Patchmaster software, on Page 92, which can be downloaded from:

http://www.heka.com/downloads/software/manual/m_patchmaster.pdf.

3. Results and Discussion

3.1. *Infrared light modulation on neuron cell*

For long-term study, CIS-980 was applied as background excitation to hippocampal neurons. During this background excitation, whole cell currents were recorded at the selected time point by patch clamp. The protocol of the depolarization pulses was routinely configured as a 10 ms holding potential followed by a 12 ms duration excitation voltage, and then ending as a 10 ms holding potential. The holding potential was −70 mV and the excitation voltages were set from −60 to 50 mV in 10 mV increments. The records were manually carried out at the concerned probe times. There existed no holding potential between each recording trial. The neuron cell was in the diameter of around ∼30 μm, which was being employed to study the infrared suppression effects.[28]

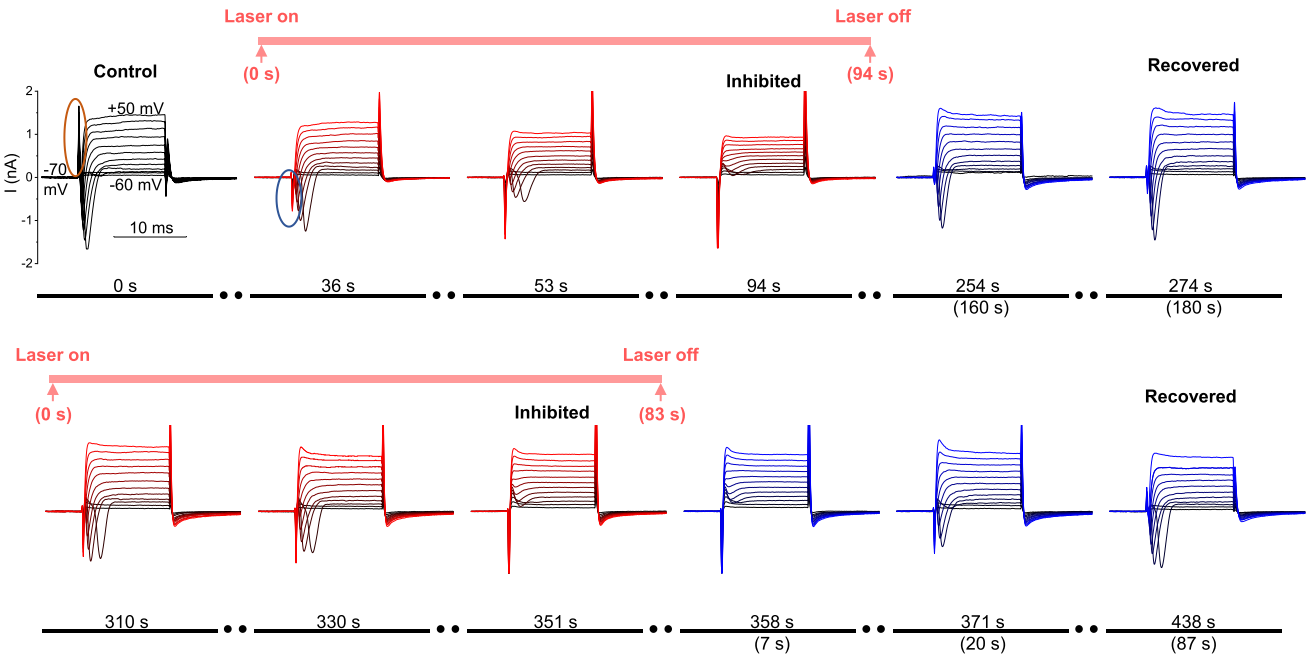

Notes: The experiment was done in two recycles of laser irradiation and indicated by red bar above the recording. In the first recycle, we found a total suppression of Na current observed after 94 s of infrared irradiation. But the K currents were little changed. Then, the light was turned off, and it was kept on waiting for about 180 s until it recovered. During this procedure, both the capacitance current and the whole cell currents were recorded. According to the time indicated above the line, the (0 s) marked the neuron cell was in the control state. We can find that the direction of the capacitance current becomes opposite from outward (positive) in control changed to inward (negative), which was indicated by the red and blue oval circle, respecively. And the same irradiation was done again in 83 s and the phenomena were repeated well. The number below the line in the bracket was the time calculated from the time of laser off.

Fig. 2. The inhibition on transmembranesodium currects on a freshly isolated hippocampal neuron cell *in vitro* with CIS-980.

The results are shown in Fig. 2. We can observe that the whole cell Na current(s) of a neuron cell *in vitro* were reversibly suppressed by a CIS-980 stimulation. Specifically, a positive capacitive current followed by both a transient Na current (I_{Na}) and outward-rectifier K current (I_{K}) was recorded and named as Control. According to the electrical model of a cell membrane, this capacitive current was determined by both the cell membrane capacitance and positive depolarization voltage, as the orange circle indicates.

After turning on CIS-980, the capacitive currents turned negative after 36 s from the beginning of the infrared stimulation, i.e., the negative membrane capacitive currents were recorded underlying the same positive depolarization voltages' excitation as that in control, as highlighted by the blue circle in Fig. 2. These capacitive currents can no longer be described by using the relationship of $C_m(\mathrm{d}V_m/\mathrm{d}t)$ exactly.

The most interesting phenomenon was that the deactivation of I_{Na} was accompanied with the increase of negative capacitance currents. The complete I_{Na} deactivation was recorded at 94 s, which was named as "Inhibited," meanwhile I_{K} changed a little. After turning off the CIS-980, it took about 3 min for both the capacitive and Na current(s) to be recovered gradually as shown in Fig. 2 at 274 s (Recovered).

Then, we turned on the CIS-980 again to repeat the experiment and kept on irradiating for 83 s (from 275 s). The second cycle (from 275 to 438 s in Fig. 2) showed similar results of whole cell currents as we observed in the first cycle. The Na current was suppressed and the capacitance currents turned negative again. Finally, "Recovered" state in Fig. 2 shows the recovered currents after turning off the laser for 87 s in the second cycle.

In summary, Na current, I_{Na}, was suppressed by infrared stimulation and its corresponding membrane capacitance currents turned to an opposite direction, from outward (positive) in control changed to inward (negative). Now, we set out to analyze its underlying mechanism in three aspects: Cell membrane capacitance increased by CIS-980 stimulation, I_{Na} being suppressed by the stimulation,

and the relationship between the capacitance increasing and I_{Na} suppression.

3.2. *Cell membrane capacitance increased by a CIS-980 stimulation*

In this part, we preliminarily presented the mechanism of the changes in the capacitive currents as circled in Fig. 2. In order to claim this mechanism, first, we need to figure out how the orange circle capacitive currents are being generated.

The software of the EPC-10 amplifier provides an interface to push a button "C-Slow" to complete a slow capacitance (C_{slow}) compensation. This operation was actually measured as a capacitance current and fed back as a compensation current, I_{com}, which was calculated by $I_{\mathrm{com}} = C_{\mathrm{slow}}(dV/dt)$ at a given excitation voltage V. Based on the compensation principle, the measured membrane capacitance currents in control states (the orange circled current, I^{c}_{measure}) can be calculated as follows:

$$I^{c}_{\mathrm{measure}} = I_r - I_{\mathrm{com}} = \frac{CdV}{dt} = \frac{(C_{\mathrm{r}} - C_{\mathrm{slow}})dV}{dt} \quad (3)$$

This compensation principle is explained in the graph presented in Fig. 3(a). I_{com} was determined based on the measurement at the last moment, and in terms of this, compensation current was generated to be subtracted from the capacitive current. In general, this subtraction cannot be made perfect, so this also provides a method to measure the membrane capacitance.

The interesting phenomenon is indicated by the blue circle in Fig. 2. A negative (inward) capacitive current had been recorded after a routine compensation. Based on the compensation principle presented in Fig. 3(a), the real membrane capacitance C_r can be figured out based on the measured capacitance current I^{c}_{measure} underlying a given excitation voltage. Therefore, the real membrane capacitance C_r can be calculated by the measured C and the reading C_{slow} as follows:

$$C_r = C + C_{\mathrm{slow}}. \quad (4)$$

In most cases, the cell membrane capacitance C_r does not change that much during the experiments; therefore, the C_{slow} can be treated as constant. So, the measured capacitance C can directly reflect the real membrane capacitance C_r.

When an infrared laser is being applied, the real membrane capacitance is increased due to thermostriction in Refs. 35–38. The measured capacitive currents underlying infrared stimulation must include the currents caused by the changing capacitance, and considering Eq. (4), Eq. (3) becomes:

$$I^{l}_{\mathrm{measure}} = [d(VC)/dt]|_{C=C_r-C_{\mathrm{slow}}} = \frac{[C_r - C_{\mathrm{slow}}]dV}{dt} + \frac{VdC_r}{dt}, \quad (5)$$

The last step was due to C_{slow} being a constant, $dC_{\mathrm{slow}}/dt = 0$.

As shown in Fig. 3(b), an increased negative capacitance current was formed by the increased C_r

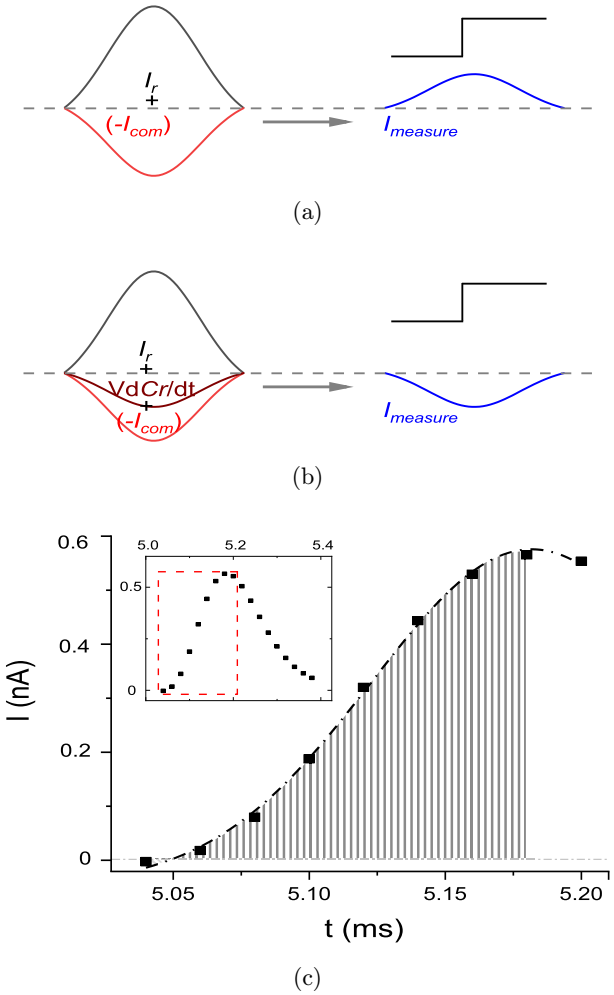

Fig. 3. The relationship between the real membrane capacitive current I_r, the compensation capacitive current I_{com}, and the measured capacitive current I_{Cm}. (a) Without infrared (Control state) capacitive current was presented as Eq. (3). (b) With infrared laser capacitive current was presented as Eq. (5). (c) The capacitive curve was fitting with a Gaussian function ($-70\,\mathrm{mV}$–$-30\,\mathrm{mV}$ at control state) to calculate the corresponding capacitive charges.

and the negative holding potential (−70 mV). This well explained the data circled in Fig. 2. When the real capacitance is being increased, a reduced capacitive current is being measured. After instead of Eq. (3) into (5), we have:

$$I^{l}_{\text{measure}} = I^{c}_{\text{measure}} + VdC_r/dt. \tag{6}$$

This prompts us to find out how large the capacitance is increased when the infrared is being applied. To evaluate it, we inserted Eq. (2) into Eq. (5) and took an integral of its both sides with the initial value as C_0, then we have:

$$\int I^{l}_{\text{measure}}dt = \frac{C(t)}{C_0}\int I^{C}_{\text{measure}}dt + \left(\frac{C(t)}{C_0} - 1\right) \times \int I_{\text{com}}dt + V_0(C(t) - C_0), \tag{7}$$

where the capacitive charges Q_{control} ($\int I^{c}_{\text{measure}}dt$), Q_{laser} ($\int I^{l}_{\text{measure}}dt$) were obtained by half integral of measured currents (details in the Appendix), which were fit by a Gauss function as shown in Fig. 3(c). The real capacitance according to time, $C(t)$, can be calculated if these charges are known. Now, we set out to calculate these charges based on the corresponding currents.

In our experiment, the reading of C_{slow} was equal to 16.87 pF, V_0 is the holding voltage −70 mV. The initial capacitance was $C_0 = 18.7$ pF, which was calculated by: $C_0 = \partial Q_{\text{control}}/\partial\Delta V + C_{\text{slow}}$. This was calculated underlying a membrane potential change as follows: $\Delta V = 10$ mV.

Aftrer inserting these values into Eq. (7), we obtained the membrane capacitance reading at $t = 36$ s was $C(t)|_{t=36\text{s}} = 19.24$ pF. Then, the temperature rise was about $\Delta T = 2.39°$C, which was calculated by instead of $t = 36$ s into Eq. (1). When considering: $dC/dT = [C(t) - C_0]/\Delta T = (19.24 - 18.7)/2.39 = 0.23$ pF/°C, the relative average temperature-dependence of capacitance changing rate during 36 s irradiation was about $dC/dT/C_0 \approx 1.23\%/°$C. The change of fast capacitance could be ignored as discussed before.[34]

3.3. *The Na current(s) being suppressed by CIS-980 stimulation*

In Fig. 2, we can find that the Na current(s) were deactivated completely but the K currents were little changed under the interaction of infrared. We performed a currents reduction normalization to quantify the difference between the two channels as follows. First, we calculated the reduction ratio of the Na current(s) compared with that in control (without CIS-980):

$$\Delta I_{\text{Na}}|\Delta V = \frac{[I_{\text{Na}}(t) - I_{\text{Na}}(0)]}{I_{\text{Na}}(0)}, \tag{8}$$

where $I_{\text{Na}}(0)$ and $I_{\text{Na}}(t)$ are corresponding to I_{Na}s recorded at control state and time t, respectively. Specifically, Na peak values recorded at 30 and 40 mV ΔV conditions are used in the estimation in Eq. (8). Figure 4(a) shows the reductions of Na channel currents at the time given in Fig. 2 and the plots together with the changes of both capacitance and K currents.

For K channel, the difference of I_{K} was extracted from the originally recorded data in Fig. 2 and is shown

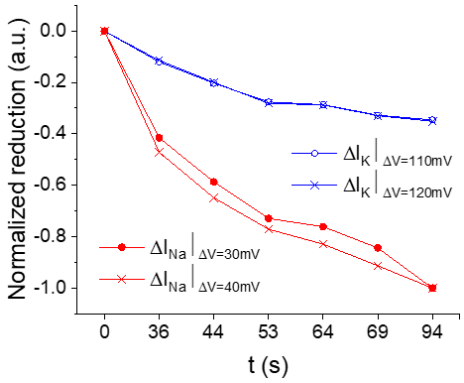

(a)

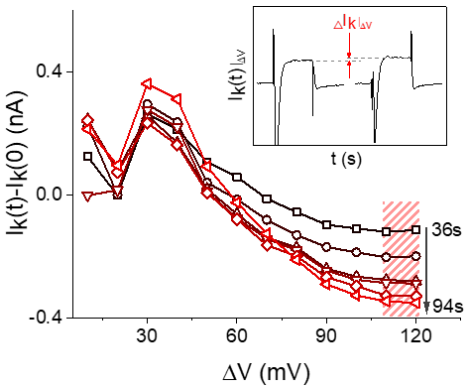

(b)

Notes: Red lines and blue lines in (a) were normalized reductions of I_{Na} peak value and K steady values. (b) K steady-state currents were obtained, where the difference between different time points reaches stability. Inset: The difference calculation method.

Fig. 4. Na and K currents decreased with radiation time in different sensitivities.

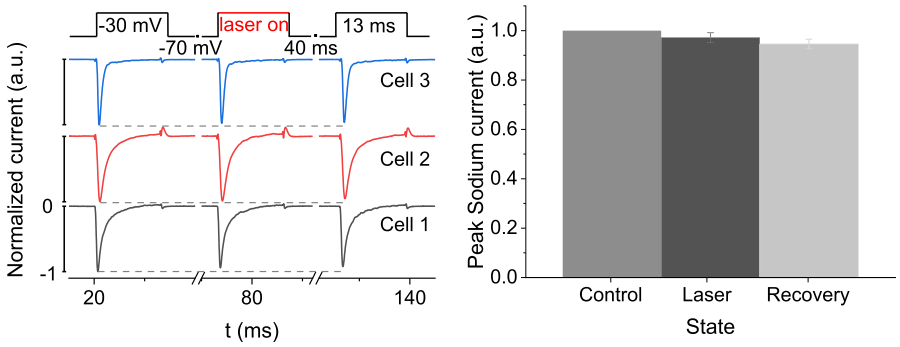

(a) (b)

Fig. 5. Short-term CIS-980 on the freshly isolated hippocampal neuron cell *in vitro*. (a) Cellular currents recorded in three cells with three segments (control, laser, recovery). (b) The statistical analysis of peak I_{Na} values according to the data presented in (a), and presented as a histogram ($N = 5$ and $P = 0.023$).

in the inset of Fig. 4(b). At 110 and 120 mV ΔV conditions, the difference became stable and we defined this value as steady value. Then, the normalized reduction of I_{K} steady values can be expressed as follows:

$$\Delta I_{\mathrm{K}}|\Delta V = \frac{[I_{\mathrm{K}}(t) - I_{\mathrm{K}}(0)]}{I_{\mathrm{K}}(0)}, \tag{9}$$

where $I_{\mathrm{K}}(0)$ was the K current in control, and $I_{\mathrm{K}}(t)$ was corresponding to the K currents recorded at the time t from the beginning of the CIS-980.

From Fig. 4(a), we found that the peak values of I_{Na} were reduced by about 60% at 44 s, and then further suppressed completely at 94 s [Fig. 4(a)], showing its sensitivity to CIS-980. I_{K} was changed little by CIS-980, meanwhile I_{Na} is completely deactivated (94 s), and the differences between their normalized reductions are increased with irradiation time.

To explore the more convincing results, we designed a short-term experiment to stimulate hippocampal neuron cells by infrared and in the condition of blocked K channel by TEA. The excitation voltage was applied from −70 mV to −30 mV as shown in Fig. 5(a). The data were divided into three segments, namely, control, laser, and recovery, respectively. At the segment "laser," the irradiation laser pulse was synchronized by the upon the edge of the depolarization voltage.

The experiments were carried out on five independent cells and three trials are shown in Fig. 5(a). There, the peak I_{Na} values of three segments were normalized in Fig. 5(b) to contrast whether the laser irradiation had suppressed the current. After calculating the ratio of the currents by laser over by control, a $P = 0.023$ was obtained. We could conclude that the I_{Na} was inhibited by CIS-980 during the "laser" stage. Furthermore, this reduction is not fully recovered after 40 ms of laser shutdown. This shows a slow recovery process, which is consistent with the gradual recovery shown in Fig. 2.

4. Discussions and Conclusions

This paper presented an experimental observation on an infrared light suppression of bioelectrical activity on the freshly isolated hippocampal neuron cell. Its mechanism can be tentatively understood both in time, whether it is rapid or not, and space, whether the energy of the infrared light spot is distributed uniform or not.

(1) The rate of the temperature changes $\mathrm{d}T/\mathrm{d}t$
It was the rate of the temperature changes induced by the infrared stimulation that determined whether the AP was suppression or enhancement. Without loss of generality, a membrane capacitance current, I_c, in a changing temperature field, T, can be expressed as follows:

$$I_c = \frac{d(VC)}{dt} = C\frac{dV}{dt} + V\frac{dC}{dt}$$
$$= C\frac{dV}{dt} + V\frac{dC}{dT}\frac{dT}{dt}, \tag{10}$$

where V is the voltage being applied to observe the capacitance current.

Combining with the cases in Refs. 8–14, we found that infrared light can regulate the neuron cell function through its capacitive current by considering the infrared-induced photothermal effect which is mediated by the capacitance changes. In the enhancement, the infrared laser is employed usually with a

wavelength $>1.5\,\mu$m, but the suppression wavelength is usually shorter. We compared 980 nm of the above results with that in Refs. 9 and 12, the absorption properties of water,[32] which is the major gradient of the biological tissue, can be very different. That of 980 nm light in water is 3.362×10^{-6} and $1.5\,\mu$m is about 1.25×10^{-4}, they are calculated by using a linear interpolation method based on the data in Ref. 32. This means the wavelength of $1.5\,\mu$m must generate much more rapid temperature changes, i.e., dT/dt becomes prominent in Eq. (10), than that of 980 nm. This is also comparable to the enhancement role in the cases of $dT/dt < 0$, when we elicit an AP right after the infrared laser irradiation is turned off as presented in Refs. 13 and 14.

On the other hand, the suppression cases will be different. In this case, a weak absorption can only generate a slow temperature rise. This could be something like a cell being applied a ramp depolarization voltage,[39] by which the deactivation process of the cell is accelerated.

(2) Infrared energy in the spot distributed uniform or not

We know that an excitable cell membrane need not have to be uniformly depolarized to evoke an AP; a localized potential increase can be enough to trigger an AP. Its counterpart means if we employed an infrared to suppress the AP generation, we must overall control the membrane potential. This is why the inhibition was effective in small-diameter axons reported in Ref. 19. The K channel mechanism underlying the suppression was not suitable to explain a general inhibition process, at least in our cases that is not the right reason.

The deeper mechanism such as acceleration of inactivation kinetics of Na channel is also an interesting topic and will be studied in the future by considering its possibility to trigger a mechanism of slow inactivation.[39] On the other hand, we will employ infrared lasers with different wavelengths, which were chosen according to their absorption coefficient in water to control their photothermal effect at an appropriate time rate. These chosen wavelengths can obtain the different rates of temperature rises in solutions and help us to understand the effect on the suppression of transmembrane Na current(s), AP, or some bioelectrical activities that existed in laser therapies, etc.

Conflicts of Interest

The authors declare that there are no conflicts of interest relevant to this paper.

Acknowledgments

This study was financially supported by the National Natural Science Foundation of China (No. 31370835) and National Science and Technology Major Special Project on new drug innovation (No. 2012ZX09503- 001-003), and funding from the Dalian University of Technology for the corresponding author (No. DUT21YG121).

Appendix A

Capacitance calculation based on measured capacitive currents

$$I^{l}_{\text{measure}} + I_{\text{com}} = C\frac{dV}{dt} + V\frac{dC}{dt},$$

$$I^{C}_{\text{measure}} + I_{\text{com}} = C_0\frac{dV}{dt},$$

$$\int I^{l}_{\text{measure}}dt = \frac{C}{C_0}\int I^{c}_{\text{measure}}dt + \left(\frac{C}{C_0} - 1\right) \times \int I_{\text{com}}dt + V\int \frac{dC}{dt}dt,$$

$$Q_{\text{laser}} = \frac{C}{C_0}Q_{\text{control}} + \left(\frac{C}{C_0} - 1\right)Q_{\text{com}} + V(C - C_0),$$

$$Q_{\text{com}} = 2 * \Delta V * C_{\text{com}},$$

$$C = \frac{Q_{\text{laser}} + Q_{\text{com}} + VC_0}{\frac{Q_c}{C_0} + \frac{Q_{\text{com}}}{C_0} + V},$$

$$\frac{dC}{dT} = (C - C_0)/\Delta T. \tag{A.1}$$

where, I^{l}_{measure} and I^{C}_{measure} were measured currents in an experiment at laser and control states, I_{com} was read from EPC-10 software, which was defined as positive with an opposite phase. C_0 was the capacitance of the neuron at the initial state, and C represented that at time t. Q_{com} was $2{*}C_{\text{slow}} * \Delta V$ because it happened twice at the same ΔV condition (control state and time t), ΔV is voltage depolarization.

References

1. Y. H. Chen, L. Q. Liu, J. C. Fan, T. R. Zhang, Y. Zeng, Z. G. Su, "Low-level laser treatment promotes skin wound healing by activating hair follicle stem cells in female mice," *Laser Med. Sci.* **37**(3), 1699–1707 (2022).
2. S. A. Tantawy, W. K. Abdelbasset, D. M. Kamel, S. M. Alrawaili, "A randomized controlled trial comparing helium–neon laser therapy and infrared laser therapy in patients with diabetic foot ulcer," *Laser Med. Sci.* **33**(9), 1901–1906 (2018).
3. A. Takenori, M. Ikuhiro, U. Shogo, K. Hiroe, S. Junji, T. Yasutaka, K. Hiroya, N. Miki, "Immediate pain relief effect of low level laser therapy for sports injuries: Randomized, double-blind placebo clinical trial," *J. Sci. Med. Sport.* **19**(12), 980–983 (2016).
4. M. Q. Yang, T. Guan, Y. H. He, "Photoacoustic effect invokes auditory response in infrared neuron stimulation," *J. Innov. Opt. Health Sci.* **12**(1), 850040 (2019).
5. R. T. Richardson, A. C. Thompson, A. K. Wise, K. Needham, "Challenges for the application of optical stimulation in the cochlea for the study and treatment of hearing loss," *Expert Opin. Biol. Ther.* **17**(2), 213–223 (2017).
6. K. Paulmurugan, V. Vijayaragavan, S. Ghosh, P. Padmanabhan, B. Gulyas, "Brain–computer interfacing using functional near-infrared spectroscopy (fnirs)," *Biosensors* **11**(10), 389–409 (2021).
7. J. Wells, C. Kao, K. Mariappan, J. Albea, E. D. Jansen, P. Konrad, A. Mahadevan-Jansen, "Optical stimulation of neural tissue *in vivo*," *Opt. Lett.* **30**(5), 504–506 (2005).
8. A. L. Hodgkin, A. F. Huxley, "A Quantitative description of membrane current and its application to conduction and excitation in nerve," *J. Physiol.* **117**(4), 500–544 (1952).
9. S. S. Liang, F. Yang, C. Zhou, Y. Wang, S. Li, C. K. Sun, J. L. Puglisi, D. Bers, C. S. Sun, J. Zheng, "Temperature-dependent activation of neurons by continuous near-infrared laser," *Cell Biochem. Biophys.* **53**(1), 33–42 (2009).
10. Q. Liu, M. J. Frerck, H. A. Holman, E. M. Jorgensen, R. D. Rabbitt, "Exciting cell membranes with a blustering heat shock," *Biophys. J.* **106**(8), 1570–1577 (2014).
11. R. D. Rabbitt, A. M. Brichta, H. Tabatabaee, P. J. Boutros, J. Ahn, C. C. Della Santina, L. A. Poppi, R. Lim, "Heat pulse excitability of vestibular hair cells and afferent neurons," *J. Neurophysiol.* **116**(2), 825–843 (2016).
12. M. G. Shapiro, K. Homma, S. Villarreal, C. P. Richter, F. Bezanilla, "Infrared light excites cells by changing their electrical capacitance," *Nat. Commun.* **3**, 736–747 (2012).
13. X. Y. Li, J. Liu, S. S. Liang, K. W. Guan, L. J. An, X. F. Wu, S. Li, C. S. Sun, "Temporal modulation of sodium current kinetics in neuron cells by near-infrared laser," *Cell Biochem. Biophys.* **67**(3), 1409–1419 (2013).
14. X. Y. Li, J. Liu, S. S. Liang, C. S. Sun, "980-nm infrared laser modulation of sodium channel kinetics in a neuron cell linearly mediated by photothermal effect," *J. Biomed. Opt.* **19**(10), 105002–105009 (2014).
15. M. Plaksin, E. Shapira, E. Kimmel, S. Shoham, "Thermal transients excite neurons through universal intramembrane mechanoelectrical effects," *Phys. Rev. X* **8**(1), 011043–011055 (2018).
16. Z. Ebtehaj, A. Hatef, M. Malekmohammad, M. Soltanolkotabi, "Computational modeling and validation of thermally induced electrical capacitance changes for lipid bilayer membranes irradiated by pulsed lasers," *J. Phys. Chem. B* **122**(29), 7319–7331 (2018).
17. R. D. Rabbitt, "The cochlear outer hair cell speed paradox," *Proc. Natl. Acad. Sci. USA* **117**(36), 21880–21888 (2020).
18. A. R. Duke, M. W. Jenkins, H. Lu, J. M. McManus, H. J. Chiel, E. D. Jansen, "Transient and selective suppression of neural activity with infrared light," *Sci. Rep.UK* **3**, 2600–2608 (2013).
19. E. H. Lothet, K. M. Shaw, H. Lu, J. Q. Zhuo, Y. T. Wang, S. Gu, D. B. Stolz, E. D. Jansen, C. C. Horn, H. J. Chiel, M. W. Jenkins, "Selective inhibition of small-diameter axons using infrared light," *Sci. Rep.* **7**, 3275–3283 (2017).
20. X. D. Zhu, J. W. Lin, M. Y. Sander, "Infrared inhibition and waveform modulation of action potentials in the crayfish motor axon," *Biomed. Opt. Exp.* **10**(12), 6580–6594 (2019).
21. Q. L. Xia, T. Nyberg, "Inhibition of cortical neural networks using infrared laser," *J. Biophoton.* **12**(7), e2018004037, 5184–5187 (2019).
22. S. Yoo, S. Hong, Y. Choi, J. H. Park, Y. Nam, "Photothermal inhibition of neural activity with near-infrared-sensitive nanotransducers," *ACS Nano* **8**(8), 8040–8049 (2014).
23. K. Eom, K. M. Byun, S. B. Jun, S. J. Kim, J. Lee, "Theoretical study on Gold-Nanorod-Enhanced

near-infrared neural stimulation," *Biophys. J.* **115**(8), 1481–1497 (2018).
24. A. L. Hodgkin, B. Katz, "The effect of temperature on the electrical activity of the giant axon of the squid," *J. Physiol.London* **109**(1–2), 240–249 (1949).
25. S. Fribance, J. Wang, J. R. Roppolo, W. C. Groat, C. Tai, "Axonal model for temperature stimulation," *J. Comput. Neurosci.* **41**, 185–192 (2016).
26. M. Ganguly, M. W. Jenkins, E. D. Jansen, H. J. Chiel, "Thermal block of action potentials is primarily due to voltage-dependent potassium currents: A modeling study," *J. Neural Eng.* **16**(3), 036020, 1–21 (2019).
27. E. Neher, B. Sakmann, "Single-channel currents recorded from membrane of denervated frog musclefibers," *Nature* **260**(5554), 799–802 (1976).
28. A. R. Kay, R. K. S. Wong, "Isolation of neurons suitable for patch-clamping from adult mammalian central nervous systems," *J. Neurosci. Meth.* **16**(3), 227–238 (1986).
29. M. J. C. Gemert, G. W. Lucassen, A. J. Welch, "Time constants in thermal laser medicine: II. Distributions of time constants and thermal relaxation of tissue," *Phys. Med. Biol.* **41**(8), 1381–1399 (1996).
30. S. Jun, R. D. Lowe, R. D. Snook, "A model for Cw laser-induced mode-mismatched dual-beam thermal lens spectrometry," *Chem. Phys.* **165**(2–3), 385–396 (1992).
31. H. Cabrera, E. Sira, K. Rahn, M. Garcia-Sucre, "A thermal lens model including the Soret effect," *Appl. Phys. Lett.* **94**, 051103–051108 (2009).
32. G. M. Hale, M. R. Querry, "Optical-constants of water in 200-nm to 200-um wavelength region," *Appl. Opt.* **12**(3), 555–563 (1973).
33. J. Yao, B. Y. Liu, F. Qin, "Rapid temperature jump by infrared diode laser irradiation for patch-clamp studies," *Biophys. J.* **96**(9), 3611–3619 (2009).
34. F. Kong, X. Li, R. Jiao, C. Sun, "Study on the temperature characteristics of fast capacitance in patch clamp experiments," *J. Biomed. Eng. (in Chinese)* **38**(4), 695–702 (2021).
35. P. Szekely, T. Dvir, R. Asor, R. Resh, A. Steiner, O. Szekely, A. Ginsburg, J. Mosenkis, V. Guralnick, Y. Dan, T. Wolf, C. Tamburu, U. Raviv, "Effect of temperature on the structure of charged membranes," *J. Phys. Chem. B* **115**(49), 14501–14506 (2011).
36. J. Pan, S. Tristram-Nagle, N. Kucerka, J. F. Nagle, "Temperature dependence of structure, bending rigidity, and bilayer interactions of dioleoylphosphatidylcholine bilayers," *Biophys. J.* **94**(1), 117–124 (2008).
37. L. K. Tamm, S. A. Tatulian, "Infrared spectroscopy of proteins and peptides in lipid bilayers," *Q. Rev. Biophys.* **30**(4), 365–429 (1997).
38. J. M. Conway, K. H. Norris, C. E. Bodwell, "A new approach for the estimation of body-composition-infrared interactance," *Am. J. Clin. Nutr.* **40**(6), 1123–1130 (1984).
39. B. Hille, *Ionic Channels of Excitable Membranes*, 3rd Edition, Sinauer Associates Sunderland, MA (2001).